ToxSci Advance Access published August 7, 2016

Title: Identification of drug-drug interactions *in vitro*: a case study evaluating the effects of sofosbuvir and amiodarone on hiPSC-derived cardiomyocytes

Running Title: Cellular effects of sofosbuvir-amiodarone

Authors: Daniel C. Millard[*], Christopher J. Strock[†], Coby B. Carlson[‡], Natsuyo Aoyama[‡], Krisztina Juhasz[§,¶], Tom A. Goetze[§], Sonja Stoelzle-Feix[§], Nadine Becker[§], Niels Fertig[§], Craig T. January[‖], Blake D. Anson[‡], Jim D. Ross[*]

Affiliations: [*]Axion BioSystems, Inc, Atlanta, GA; [†]Cyprotex, Watertown, MA; [‡]Cellular Dynamics International, a Fujifilm Company, Madison, WI; [§]Nanion Technologies GmbH, Munich, Germany, [¶]Technische Universitat Munchen, Munich, Germany; [‖]School of Medicine and Public Health, University of Wisconsin, Madison, WI

Manuscript Word Count: 6040

Supplemental Word Count: 530

Address correspondence to:

Daniel C. Millard
Axion BioSystems, Inc
1819 Peachtree Road NW
Suite 350
Atlanta, GA 30309
(919)244-8279
dmillard@axion-biosystems.com

Abstract

Drug-drug interactions pose a difficult drug safety problem, given the increasing number of individuals taking multiple medications and the relative complexity of assessing the potential for interactions. For example, sofosbuvir-based drug treatments have significantly advanced care for hepatitis C virus-infected patients, yet recent reports suggest interactions with amiodarone may cause severe symptomatic bradycardia and thus limit an otherwise extremely effective treatment. Here, we evaluated the ability of human induced pluripotent stem cell derived cardiomyocytes (hiPSC-CMs) to recapitulate the interaction between sofosbuvir and amiodarone *in vitro*, and more generally assessed the feasibility of hiPSC-CMs as a model system for drug-drug interactions. Sofosbuvir alone had negligible effects on cardiomyocyte electrophysiology, whereas the sofosbuvir-amiodarone combination produced dose-dependent effects beyond that of amiodarone alone. By comparison, GS-331007, the primary circulating metabolite of sofosbuvir, had no effect alone or in combination with amiodarone. Further mechanistic studies revealed that the sofosbuvir-amiodarone combination disrupted intracellular calcium (Ca^{2+}) handling and cellular electrophysiology at pharmacologically relevant concentrations, and mechanical activity at supra-pharmacological (30x C_{max}) concentrations. These effects were independent of the common mechanisms of direct ion channel block and P-glycoprotein activity. These results support hiPSC-CMs as a comprehensive, yet scalable model system for the identification and evaluation of cardioactive pharmacodynamic drug-drug interactions.

Keywords: Cardiomyocyte, Cardiac Electrophysiology, Stem Cell, Safety, Drug Interactions

Non-standard Abbreviations and Acronyms:

hiPSC-CM	Human Induced Pluripotent Stem Cell Derived Cardiomyocyte
MEA	Microelectrode Array
APC	Automated Patch Clamp
IMP	Impedance
BP	Beat Period
FPD	Field Potential Duration
FPDc	Field Potential Duration, Corrected
AMP	Spike Amplitude
CaI	Calcium Imaging
P-gp	P-glycoprotein

Introduction

Drug-drug interactions pose a difficult drug safety problem, given the increasing number of individuals taking multiple medications (Hajjar *et al.*, 2007) and the relative complexity of assessing the potential for interactions (Prueksaritanont *et al.*, 2013). While investigations into pharmacokinetic drug-drug interactions are now routine *in vitro* and in clinical trials (Bjornsson *et al.*, 2003), pharmacodynamic drug-drug interactions are impractical to evaluate in clinical trials and generally undetectable with reduced *in vitro* preparations designed for high throughput screening.

Within cardiovascular safety pharmacology, a long history of drug-drug interactions exists for cardiovascular drugs (Hager *et al.*, 1979; Nutescu *et al.*, 2011; Anderson and Nawarskas, 2001). Indeed, the high degree of polypharmacy (Hajjar *et al.*, 2007), and cardiovascular drug usage (Gurwitz *et al.*, 2003), in the elderly has led to a significant issue with cardiovascular drug-drug interactions (Köhler *et al.*, 2000; Straubhaar *et al.*, 2006). Recent reports have utilized statistical models in an attempt to predict potential drug-drug interactions with electrophysiological cardiac effects (Lorberbaum *et al.*, 2016), but the ability to reproduce, and ultimately screen for, pharmacodynamic drug-drug interactions *in vitro* has not been demonstrated.

Human induced pluripotent stem cell derived cardiomyocytes (hiPSC-CMs) may provide a model for assessing cardiac drug-drug interactions, as these cells are amenable to high throughput *in vitro* investigations and recapitulate key features of human cardiac electrophysiology. Robust evaluation of potential drug-induced cardiac safety liabilities, created by altered electrophysiology and mechanical activity, can be achieved through a variety of functional hiPSC-CM assays (Doerr *et al.*, 2015; Harris *et al.*, 2013; Guo *et al.*, 2013; Gilchrist *et al.*, 2015). In addition, the comprehensive nature of hiPSC-CMs may enable further mechanistic insight into known or anticipated drug-drug interactions with cardiac effects.

The drug-drug interaction between sofosbuvir and amiodarone serves as a recent example of an unanticipated interaction with cardiac effects. Sofosbuvir-based drugs have significantly advanced care for hepatitis C virus-infected patients (Lawitz *et al.*, 2014; Jacobson *et al.*, 2013; Keating, 2014). Although sofosbuvir did not exhibit adverse cardiac activity in clinical trials (Lawitz *et al.*, 2013), recent post-marketing reports indicate that severe symptomatic bradycardia can occur through combined administration of sofosbuvir and amiodarone (Renet *et al.*, 2015; FDA, 2015). The underlying mechanistic consequences of this drug-drug interaction remain unknown, but recent hypotheses suggest an interaction with the p-glycoprotein (P-gp) drug transporter (Soriano *et al.*, 2015; Back and Burger, 2015).

Here, we present a multifaceted interrogation of the cellular effects of sofosbuvir and amiodarone on hiPSC-CMs. Microelectrode array (MEA) recordings demonstrated that sofosbuvir and amiodarone interact to affect hiPSC-CM electrophysiology. The electrophysiological effects elicited by the drug-drug interaction were not caused by the more commonly observed mechanism of direct block of sodium, potassium, or calcium currents, inhibition of the P-gp drug transporter, or metabolite production. Rather, the electrophysiological effects were associated with a disruption of intracellular calcium handling at clinically relevant concentrations, and cessation of contractile beating at the highest supra-physiological concentrations, indicating a pharmacodynamic drug-drug interaction with a cardiac mechanism of action. The results from these presented experiments provide new mechanistic insight into the sofosbuvir-amiodarone interaction, and more generally suggest that hiPSC-CMs could serve as a comprehensive model system for evaluating cardioactive pharmacodynamic drug-drug interactions.

Materials and Methods

The individual and combinatorial effects of sofosbuvir and amiodarone on hiPSC-CMs were evaluated using MEA, impedance (IMP), and calcium imaging (CaI) assays. The iCell Cardiomycytes[2] (Cellular Dynamics International; CDI) were used for all cardiomyocyte-based assays in this study. All cell and instrument handling was done per manufacturer instructions, as described below. Drug doses were based on the reported C_{max} value for sofosbuvir, 1.14µmol/L (Lawitz *et al.*, 2013), and the minimum effective plasma steady-state concentration of amiodarone, 0.57µmol/L (Latini *et al.*, 1984). All error bars represent standard deviations.

Automated Patch Clamp

Standard cell line culture. The overexpressed ion channel cell lines (Cav1.2/β2/α2δ-CHO, no. CT6004; Nav1.5 CHO, no. CT6007; Kv11.1 (hERG) HEK293, no. CT6001, all from Chantest) were cultured as previously described (Becker *et al.*, 2013; Bruggemann *et al.*, 2009; Obergrussberger *et al.*, 2014). In brief, cells were cultured in T75 culture flasks in manufacturer recommended media and passaged at 50-80% confluency (every 2 – 3 days) to ensure a healthy suspension of completely dissociated cells prior to recording. Cells were harvested as described previously using trypsin, other suitable enzymes, or even enzyme-free detachment protocols (Becker *et al.*, 2013; Obergrussberger *et al.*, 2014; Bruggemann *et al.*, 2009). Cells were then re-suspended in a mixture of 50% culture media/50% external recording solution at a density of 50,000 – 500,000 cells per ml.

Patch Clamp Solutions. Internal solution for hERG: 50 mmol/L KCl, 10 mmol/L NaCl, 60 mmol/L KF, 20 mmol/L EGTA, 10 mmol/L HEPES/KOH, pH 7.2. Internal solution for Nav1.5 experiments: 10 mmol/L CsCl, 110 mmol/L CsF, 20 mmol/L EGTA, 10 mmol/L HEPES/CsOH, pH 7.2. Internal solution for Cav1.2 experiments: 120 mmol/L CsF, 20 mmol/L KCl, 10 mmol/L NaCl, 2mmol/L MgCl, 2mmol/L EDTA, 5 mmol/L EGTA, 10 mmol/L Hepes, pH7.2, 1 mmol/L Na-ATP, 25 µmol/L Escin. External recording solution for Nav1.5 and hERG: 140 mmol/L NaCl, 4 mmol/L KCl, 1 mmol/L MgCl2, 2 mmol/L CaCl2, 5 mmol/L D-Glucose monohydrate, 10 mmol/L HEPES/NaOH pH 7.4. External solution for Cav1.2: 80 mmol/L NaCl, 60 mmol/L NMDG, 4 mmol/L KCl, 2 mmol/L CaCl2, 1 mmol/L MgCl2, 5 mmol/L Glucose, 10 mmol/L HEPES, pH 7.4.

Electrophysiology. All cells were recorded in the whole cell patch clamp mode using the Patchliner or the SyncroPatch 384PE (Nanion Technologies) incorporated into a Biomek FX pipetting robot (Beckman Coulter). hERG recordings were performed at 35°C, all other recordings at room temperature. Cells were added to the patch clamp recording chips and attached to the aperture of each well by suction when necessary. Voltage protocols were constructed and data acquired using PatchMaster (HEKA Elektronik) or PatchControl 384 (Nanion Technologies).

Microelectrode Array

Cell Culture. iCell Cardiomycytes[2] were used for the microelectrode array (MEA) recordings acquired using the Maestro multiwell electrophysiology platform (Axion BioSystems, Inc.). Cells were plated according to cell manufacturer recommendations. Briefly, a 5µL drop of fibronectin was applied to the electrode array of each well and allowed to incubate for one hour at 37°C. Cardiomyocytes were thawed, centrifuged, and resuspended to 10^7 cells/mL. The fibronectin was then aspirated from each well and replaced with a 5µL drop of the cell suspension (~50k cells/well). The plate was incubated for one hour at 37°C and then 300µL of iCell Maintenance Media (iCMM) added to each well.

Experimental Protocol. The media was changed at least two hours prior to the experiment to minimize the effect of thermal, mechanical, or chemical perturbations on the cells. On the day of the experiment,

the cell culture plate was moved directly from the incubator to the MEA device for a baseline recording (30min), with environmental controls (37°C and 5% CO_2) used to maintain the temperature and pH.

A single dosing scheme was utilized, such that each MEA well received only one dose of a particular compound or compound mixture. Compounds were prepared on the day of use at 10x the final concentration, stored in at 37°C and 5% CO_2 until the dosing (no more than 4 hours after formulation). Wells were dosed by removing 10% of the media volume and replacing with the same volume of the prepared compound (at 10x the final concentration). The MEA wells were dosed in a biosafety cabinet, restored to the MEA device, environmental controls re-engaged, and allowed to equilibrate for ~30min. Spontaneous cardiac electrical rhythms were recorded continuously during the equilibration period.

Data Analysis. Three primary endpoints were derived from the cardiac field potential (FP) in the baseline and post-dose conditions: 1) spike amplitude (AMP), 2) field potential duration (FPD), and 3) beat period (BP). An example of the cardiac field potential, and the associated measurement definitions, is shown in Suppl. Fig. 1. The onset of cardiac depolarization is marked by a sharp deflection in the field potential signal, termed the depolarization spike. Depolarization spike AMP provides a measure of the speed of depolarization in the cardiomyocyte network. FPD is given by the timing interval between the depolarization spike and the peak of the repolarization feature. BP was defined as the duration between two consecutive depolarization spikes.

The baseline and post-dose measurements were taken during the five minutes immediately following the equilibration period. All analysis was performed using the Axion Integrated Studio (AxIS) software suite (Axion BioSystems, Inc) where an algorithm used BP to identify the most stable continuous string of 30 beats. These beats were then used to compute the average AMP, FPD, and BP metrics. Baseline and post-dose FPD measurements were rate corrected (FPDc) using the Fridericia correction (Fridericia, 1920); subsequently, the percent change from baseline to post-dose was calculated for each well.

Optogenetic Pacing. For the pacing experiment, the cells were transduced by adding 9µL of the viral vector construct (AAV9-ChR2-CAG-GFP, UNC Viral Vector Core) to a cell suspension prepared for 24-wells before seeding the cells on the MEA as described above. The pacing experiment was performed 12 days after transduction to allow sufficient time for expression of the light sensitive channel (opsin). The cells were paced using 5ms pulses of blue light (470nm) from a multiwell light delivery device (Lumos, Axion BioSystems, Inc). Measurements were made after the FPD had stabilized at the paced beating rate.

Calcium Imaging

Cell culture. Cryopreserved iCell Cardiomyocytes[2] were thawed and cultured according to the manufacturer recommended protocol with cardiomyocytes seeded at a density of ~16,000 live cells per well in 33µL of iCell CM plating medium (iCPM) in black 384-well plates (Greiner Bio-one) coated with 0.1% gelatin. After 4hr, iCPM was exchanged to 40µL of iCMM with media changes every other day until the day of the assay.

Experimental Protocol. On Day 7 post-thaw, media was aspirated and replaced with 20µL of iCMM and cells were loaded with 20µL of the 2X calcium dye from the EarlyTox Cardiotoxicity Kit (Molecular Devices) for 2hr in the incubator. Cells were treated with 10µL of 5x compound titrations (or DMSO control) prepared in iCMM and further incubated for 30min. Assay plates were then read on the FDSS/µCell at 37°C.

Data Analysis. The amplitude of the fluorescence signal was computed by automated software (Hamamatsu) for each well on the plate, and then the percent change from baseline to post-dose was calculated before averaging across replicate wells.

Impedance

Cell culture. iCell Cardiomyocytes^2 were seeded at a density of 50,000 cells per well on a CardioExcyte 96 sensor plate (Nanion Technologies) according to cell manufacturer recommendations. The 96-well sensor plates were coated with fibronectin (Sigma Aldrich; 1:100 solution in phosphate-buffered saline without Ca^{2+}/ Mg^{2+}) and kept for 1.5hr in the incubator (37°C, 5% CO_2). A cell suspension of 500 viable cells/µl was prepared from thawed iCell Cardiomyoctes^2. After removing the fibronectin solution, 100µl pre-warmed 37°C iCPM and then the cell suspension were added to each well. The sensor plate was incubated at 37°C, 5 % CO_2 for 24hr. After that, the medium was exchanged every 2 to 3 days with iCMM.

Experimental Protocol. The medium was changed at least 2hr prior to the experiment to minimize artifacts. A single dosing scheme was applied, such that each well received only one dose of a compound. Compounds were prepared in medium containing 0.3% DMSO on the day of the experiment at 2x the final concentration and kept at 37°C until use. Wells were dosed under sterile conditions by removing 50% of the medium and replacing it by the same volume of the compound (at 2x the final concentration). The sensor plates were returned to the incubator immediately after dosing. Data were recorded continuously until 240min post-dosing. Sampling rate was 1kHz for impedance and 10kHz for field potential (FP), and sweep lengths were 10s.

Data Analysis. The software calculated the average beat shape based on the data of one sweep, termed the Mean Beat, which was used for the analysis of signal amplitudes (peak-to-peak amplitude for impedance signals; peak-to-peak amplitude of depolarization spike for FP signals).

Results

Sofosbuvir exerts an electrophysiological effect in combination with amiodarone in vitro

The individual and combinatorial effects of sofosbuvir and amiodarone on hiPSC-CMs were assessed via extracellular MEA experiments (see Methods, Suppl. Fig. 1). Figure 1 shows the effect on the raw field potential (FP), spontaneous beat period (BP), field potential duration (FPD), corrected field potential duration (FPDc, Fridericia correction), and depolarization amplitude (AMP).

The raw FP traces in Fig. 1A qualitatively illustrate that the vehicle control (gray, 0.2% DMSO) and sofosbuvir alone (green, 31.6µmol/L) at ~30x C_{max} were without effect. Dose-dependent changes are quantified in Fig. 1B, where sofosbuvir alone did not have a significant effect on BP, FPD, FPDc, or AMP across the tested concentrations, which extend 1.5 orders of magnitude above the clinical C_{max} (Fig. 1B).

Amiodarone (red, 0.6µmol/L) produced an expected prolongation in the raw FP trace (Fig. 1A), whereas the sofosbuvir-amiodarone combination (blue, 31.6µmol/L sofosbuvir, 0.6µmol/L amiodarone) elicited a marked change in the FP trace. The FP metrics were quantified for the amiodarone-sofosbuvir combination using the same escalating concentrations of sofosbuvir with a fixed concentration of amiodarone (Fig 1C). Amiodarone alone (0.6µmol/L) prolonged BP by 15.0±6.3%, FPD by 18.7±3.9%, and FPDc by 13.3±2.3%, while reducing AMP by 61.0±15.9%, as indicated by the red horizontal bars. Sofosbuvir addition eliminated, and then reversed, the effects of amiodarone in a concentration-dependent manner, with significant changes beginning at the clinical C_{max}. At the highest concentration of sofosbuvir, the drug combination shortened BP by 49.2±5.1%, FPD by 52.9±5.7%, and FPDc by 41.0±5.3% compared to baseline, while causing a 13.3±16.6% increase in AMP (* denotes $p<0.05$ between amiodarone and sofosbuvir-amiodarone doses, N=4, Wilcoxon rank-sum test).

The electrophysiological effects of the drug combination remained over chronic exposures, but recovered after wash-out (Suppl. Fig. 2). Quinidine, another P-gp inhibitor like amiodarone, did not interact with sofosbuvir in the MEA assay, nor did amiodarone alter sofosbuvir uptake into cardiomyocytes according to mass spectrometry measurements (see Suppl. Results).

GS-331007, the predominant metabolite of sofosbuvir, does not interact with amiodarone in vitro

GS-331007 is the primary metabolite of sofosbuvir and accounts for the majority of systemic exposure following a single oral dose of sofosbuvir (Gilead Sciences Inc., 2013). Importantly, however, the metabolism of sofosbuvir occurs in the liver, and thus should not occur with hiPSC-CMs *in vitro*. Therefore, to ensure this study examined the relevant chemical structure, GS-331007 and amiodarone were evaluated, using the MEA assay.

The results, illustrated in Fig. 2, indicate that GS-331007 does not impact hiPSC-CM electrophysiology when delivered alone, or in combination with amiodarone, at any tested concentration (0.1x – 10x C_{max}). None of the endpoints showed a significant change from baseline at any concentration of GS-331007 applied to the cells (Fig. 2B), consistent with the example trace in Fig. 2A (cyan). The addition of GS-331007 with amiodarone (magenta) did not affect BP, FPD, or FPDc beyond using amiodarone alone (Fig. 2C). At the highest supra-physiologic concentrations of GS-331007 (3x and 10x the C_{max}), the drug combination produced a subtle, but statistically relevant, recovery in AMP, as compared to amiodarone alone (N=4, $p<0.05$, Wilcoxon rank sum test).

The sofosbuvir-amiodarone combination shortens field potential duration independent of beating rate

The cardiomyocytes were paced to isolate changes in repolarization from changes in the spontaneous beating rate. A light sensitive ion channel, channelrhodopsin-2 (ChR2), was targeted to the cardiomyocytes, as described above, to allow optical pacing of the cardiomyocytes (Bruegmann *et al.*, 2010). An example of the onset of pacing is shown in Fig. 3A. The BP was immediately entrained by the blue light pulse stimulus (Fig. 3A) and the FPD slowly approached a new steady state value at the paced rate. Measurements of FPD were extracted after three minutes of continuous pacing to ensure stabilization. All wells were paced to a BP of 500ms because the sofosbuvir and amiodarone combination decreased the spontaneous BP to ~700ms, and cardiomyocytes cannot be entrained to a BP that is longer than the spontaneous BP.

Example paced FP waveforms are shown in Fig. 3B, with the results summarized in Fig. 3C. All paced results were similar to those obtained from spontaneous FP waveforms. Sofosbuvir (green) did not produce a significant change in FPD (0.2+/-5.7%, N=4, Wilcoxon rank sum test) compared to the vehicle control (gray, -4.7+/-2.4%, N=4) when paced at 2Hz. Amiodarone (red) caused a significant prolongation in FPD (9.2+/-7.4%, N=4, $p<0.05$, Wilcoxon rank sum test), whereas the sofosbuvir and amiodarone combination (blue) significantly reduced FPD (-21.3+/-7.8%, N=4, $p<0.05$, Wilcoxon rank sum test) in the paced condition.

The effect of sofosbuvir with amiodarone is not mediated by block of potassium, sodium, or calcium channels

Amiodarone is known to block potassium (I_{Kr}), sodium (I_{Na} and $I_{Na,late}$), and calcium (I_{CaL}) currents, consistent with the prolongation of FPD and reduction in AMP observed in these and other MEA experiments(Gilchrist *et al.*, 2015). The combination of amiodarone and sofosbuvir shortened FPD and BP, a phenotype commonly observed with I_{CaL} blockade (Clements and Thomas, 2014; Harris *et al.*,

2013; Braam *et al.*, 2010). APC experiments with simple overexpression cell lines were used to determine if direct ion channel block underlay the electrophysiological effects of sofosbuvir-amiodarone.

Figure 4A-C depict raw voltage clamp traces and summarized data for cells overexpressing channels encoded by (A) hERG, (B) Nav1.5, and (C) Cav1.2. The raw waveforms display current block by sofosobuvir-amiodarone, while the bar plots illustrate the effects of the sofosobuvir-amiodarone combination over those of amiodarone alone. Specifically, amiodarone alone (0.5µmol/L) caused 96±3% block of I_{Kr}, 22±3% block of peak I_{Na}, and 12±9% block of I_{CaL}. In combination with amiodarone, sofosbuvir at 31.6µmol/L (30xCmax) did not further impact the effects of amiodarone on I_{Kr} or I_{Na}, and showed a statistically relevant, but small, increase in I_{CaL} block ($p<0.05$, N=13-24, unpaired t-test) at only one of four amiodarone concentrations tested (Fig. 4D).

Intracellular calcium handling is impaired by sofosbuvir and amiodarone in hiPSC-CMs

Shortening of the field potential duration is commonly associated with direct I_{CaL} block, and yet the drug combination did not show a clear I_{CaL} block in the automated patch clamp experiments. I_{CaL} and the plateau phase of the cardiac action potential may also be affected by alterations in intracellular calcium handling (Bers, 2002). Therefore, the effects of sofosbuvir and amiodarone on intracellular calcium handling were evaluated using high throughput calcium imaging.

In Figure 5A, the raw calcium transient traces show minimal effect of DMSO (0.1%) and sofosbuvir (3µmol/L) and a modest effect of amiodarone (0.5µmol/L) on intracellular calcium handling (Fig. 5A). Sofosbuvir by itself continued to have no effect over a wide range of doses (Fig. 5B), but, in the presence of amiodarone, caused a marked dose-dependent decrease in the intracellular Ca^{2+} transients at clinical concentrations, and virtually complete elimination of the transient at supra-physiologic concentrations greater than or equal to 10µmol/L (Fig. 5C).

The sofosbuvir and amiodarone combination disrupts excitation-contraction coupling in vitro

Decreases in cardiomyocyte intracellular Ca^{2+} are commonly associated with downstream consequences on mechanical activity (Bers, 2002). We evaluated this possibility by monitoring the physical movement of the cardiomyocytes with IMP measurements (Guo *et al.*, 2013).

As expected, supra-physiologic concentrations of the sofosbuvir-amiodarone combination decreased cardiomyocyte mechanical activity over the same time period as the MEA and calcium recordings (Fig. 6A), while time-matched controls were unaffected (N=3, Fig. 6B). Thirty minutes after the addition of the sofosbuvir-amiodarone combination (blue, 31.6µmol/L sofosbuvir, 0.5µmol/L amiodarone), the beating frequency increased and the IMP signal decreased. Within 120 min, the mechanical activity had completely ceased.

The FP was recorded simultaneously with the IMP measurements, revealing a break in excitation-contraction coupling as the electrophysiological activity remained after the cessation of mechanical activity (N=3, Fig. 6C). Neither amiodarone nor sofosbuvir alone decoupled excitation and contraction.

Discussion

Four independent labs demonstrated signal disruption in networked hiPSC-CMs with co-administration of sofosbuvir and amiodarone, supporting the robust nature of the drug-drug interaction and reproducibility of the cellular effect. Sofosbuvir and amiodarone shortened cardiomyocyte FPD and BP and impaired intracellular Ca^{2+} handling at physiologically relevant drug concentrations, while myocyte contraction was virtually eliminated at the highest, supra-physiologic concentration tested. Additional experiments

confirmed that these effects were due to sofosbuvir and not GS-331007, the primary circulating metabolite.

A common hypothesis for drug-induced changes in cardiac electrophysiology is direct ion channel block. In this case, experimental evidence with simple heterologous channel expression systems—comprising the likely targets of hERG, Nav1.5, or Cav1.2 channels—did not support this hypothesis for the sofosbuvir-amiodarone effect. Instead, the data shown here suggest a primary effect on intracellular calcium handling at clinically relevant concentrations, which could be due to other cellular mechanisms, such as altered second messenger signaling, membrane depolarization, or disruption of sarcoplasmic calcium release, which then influence electrical activity (Bers, 2002). Thus, further mechanistic information might be achieved with follow-up studies focused on key components of intracellular calcium cycling such as the ryanondine receptor (RYR2) or calsequestrin (CASQ2), which are implicated in catecholaminergic polyventricular tachycardia (CPVT) (Postma *et al.*, 2005), or the sodium-potassium ATP-ase, which mediates the effect of cardiac glycosides (Ten Eick and Hoffman, 1969). CPVT and cardiac glycosides are both linked to bradycardia clinically, but CPVT also leads to ventricular tachycardia under adrenergic stimulation and cardiac glycosides exhibit tachycardia in iPSC-derived cardiomyocytes (Guo *et al.*, 2013; Gilchrist *et al.*, 2015).

Irrespective of the exact molecular mechanism, these *in vitro* results provide compelling evidence for a cardiac mechanism of action. Inhibition of P-glycoprotein (P-gp) mediated-drug transport is a common cause of drug-drug interactions and has been postulated in the case of sofosbuvir and amiodarone co-administration (Back and Burger, 2015; Soriano *et al.*, 2015), where P-gp block would lead to increased intracellular concentrations of the victim drug (sofosbuvir) and underlie the adverse event. Such a mechanism is unlikely in this case as sofosbuvir did not have an effect at concentrations 30-fold higher than C_{max}, in combination with other P-gp inhibitors such as quinidine, and did not show increased intracellular concentrations in the presence of amiodarone as determined by mass spectrometry studies.

While the combination of amiodarone and sofosbuvir demonstrated a clear and reproducible effect *in vitro*, a preliminary interpretation of the data shows a significant deviation from the clinical observations. However, viewing the *in vitro* and clinical data in the context of their respective underlying systems biology reveals concordant mechanisms and enables relevant translation of the experimental data. The MEA results revealed increased beat rate and shortened field potential duration at physiologic concentrations, whereas all nine reported clinical cases presented as bradycardia, with one patient entering fatal cardiac arrest (FDA, 2015). These seemingly disparate drug-induced phenotypes may be explained by examining the effects of reduced Ca^{2+} function under native and *in vitro* conditions.

Cardiac activity under normal, native conditions in the intact heart is driven by Ca^{2+} channel-mediated depolarization and conduction in the spatially-segregated sinoatrial (SA) and atrioventricular (AV) nodes (Katz, 1993). Nodal activity is then spread to, and determines the rate of, electrical activity in downstream atrial and ventricular cells. Reduced Ca^{2+} channel activity under these conditions slows nodal depolarization and electrical conduction and can thus lead to bradycardia in downstream atrial and ventricular cells (DeWitt and Waksman, 2004; Katz, 1993). hiPSC-CM monolayers, on the other hand, do not have a spatial segregation of the mixed cardiomyocyte-subtypes, such that depolarization and conduction is driven by Na^{+} channel activity with Ca^{2+} channel activity primarily influencing the plateau phase of the action potential (Ma *et al.*, 2011). Reduced Ca^{2+} channel activity under these conditions, thus leads to a shortened action potential duration and tachycardia-like activity (Clements and Thomas, 2014; Harris *et al.*, 2013; Braam *et al.*, 2010). In this way, by taking the differing systems biology into account, mechanistic precedent exists for linking clinical bradycardia to *in vitro* tachycardia in the context

of cellular calcium channel activity. More generally, it is important to consider mechanistic information when assessing the directionality of response in reduced *in vitro* model systems.

Sofosbuvir-amiodarone combination likely exhibited a pharmacodynamic drug-drug interaction. Adverse drug-drug interactions have clear clinical, financial, and societal consequences and thus illustrate a potential need for better prediction of such effects prior to full market release. The sheer number of pharmaceuticals in current use prohibits clinical investigation of drug-drug interactions, but the throughput of hiPSC-CM assays could enable cost-effective, directed assessment of cardioactive pharmacodynamic drug-drug interactions. For example, it would only require a few plate-based tests to profile a compound of interest against a library of 50 commonly prescribed or targeted drugs in an assay of hiPSC-CM functional electrophysiology with a multiwell MEA platform.

The collective *in vitro* observations provide specific evidence for a cellular mechanism related to altered cardiomyocyte calcium handling when amiodarone and sofosbuvir are co-administered. This data provides novel information by demonstrating that the sofosbuvir-amiodarone response is independent of common pharmacodynamic and pharmacokinetic interactions on ion channel activity, P-gp function, and metabolite production. Furthermore, this work illustrates how to reconcile seemingly disparate *in vitro* and clinical results and emphasizes the need to take differing systems biology into account when doing so. Ultimately, these results demonstrate the importance of measuring multiple endpoints within an intact biologically relevant model and, more generally, reinforce the utility of hiPSC-CMs for scalable integrated assessments of cardiac safety liability *in vitro*.

Acknowledgments

The authors would like to acknowledge Paula Ross, Anthony Nicolini, and Colin Arrowood for their contributions to the manuscript.

Funding Information

None of the authors received funding for the research, authorship, and/or publication of this article.

Disclosures

With the exception of CTJ, the authors are employed by either Axion BioSystems, Cellular Dynamics International, Cyprotex, or Nanion Technologies.

References

Anderson, J.R. and Nawarskas, J.J. (2001) Cardiovascular drug-drug interactions. *Cardiol. Clin.*, **19**, 215–34, v.

Back, D.J. and Burger, D.M. (2015) Interaction Between Amiodarone and Sofosbuvir-based Treatment for Hepatitis C Virus Infection: Potential Mechanisms and Lessons to be Learned. *Gastroenterology*, **149**, 1315–1317.

Becker, N. *et al.* (2013) Minimized cell usage for stem cell-derived and primary cells on an automated patch clamp system. *J. Pharmacol. Toxicol. Methods*, **68**, 82–87.

Bers, D.M. (2002) Cardiac excitation-contraction coupling. *Nature*, **415**, 198–205.

Bjornsson, T.D. *et al.* (2003) The conduct of in vitro and in vivo drug-drug interaction studies: a Pharmaceutical Research and Manufacturers of America (PhRMA) perspective. *Drug Metab. Dispos.*, **31**, 815–32.

Braam, S.R. *et al.* (2010) Prediction of drug-induced cardiotoxicity using human embryonic stem cell-derived cardiomyocytes. *Stem Cell Res.*, **4**, 107–16.

Bruegmann, T. *et al.* (2010) Optogenetic control of heart muscle in vitro and in vivo. *Nat. Methods*, **7**, 897–900.

Bruggemann, A. *et al.* (2009) Planar patch clamp: advances in electrophysiology. *Methods Mol Biol.*, **491**, 165–176.

Clements, M. and Thomas, N. (2014) High-Throughput Multi-Parameter Profiling of Electrophysiological Drug Effects in Human Embryonic Stem Cell Derived Cardiomyocytes Using Multi-Electrode Arrays. *Toxicol. Sci.*

DeWitt, C.R. and Waksman, J.C. (2004) Pharmacology, pathophysiology and management of calcium channel blocker and beta-blocker toxicity. *Toxicol. Rev.*, **23**, 223–238.

Doerr, L. *et al.* (2015) New easy-to-use hybrid system for extracellular potential and impedance recordings. *J. Lab. Autom.*, **20**, 175–88.

Ten Eick, R.E. and Hoffman, B.F. (1969) Chronotropic effect of cardiac glycosides in cats, dogs, and rabbits. *Circ. Res.*, **25**, 365–78.

FDA (2015) FDA warns of serious slowing of the heart rate when antiarrhythmic drug amiodarone is used with hepatitis C treatments containing sofosbuvir (Harvoni) or Sovaldi in combination with another Direct Acting Antiviral drug. *FDA Drug Saf. Commun.*

Fenner, K. *et al.* (2009) Drug–Drug Interactions Mediated Through P-Glycoprotein: Clinical Relevance and In Vitro–In Vivo Correlation Using Digoxin as a Probe Drug. *Clin. Pharmacol. & Ther.*, **85**, 173–181.

Fridericia, L.S. (1920) Die Systolendauer im Elektrokardiogramm bei normalen Menschen und bei Herzkranken. *Acta Med. Scand.*, **53**, 469–486.

Gilchrist, K.H. *et al.* (2015) High-throughput cardiac safety evaluation and multi-parameter arrhythmia profiling of cardiomyocytes using microelectrode arrays. *Toxicol. Appl. Pharmacol.*

Gilead Sciences Inc. (2013) Sovaldi (sofosbuvir) tablets, for oral use: US prescribing information.

Guo, L. *et al.* (2013) Refining the human iPSC-cardiomyocyte arrhythmic risk assessment model. *Toxicol. Sci.*, **136**, 581–94.

Gurwitz, J.H. *et al.* (2003) Incidence and preventability of adverse drug events among older persons in the ambulatory setting. *JAMA*, **289**, 1107–16.

Hager, W.D. *et al.* (1979) Digoxin-Quinidine Interaction. *N. Engl. J. Med.*, **300**, 1238–1241.

Hajjar, E.R. *et al.* (2007) Polypharmacy in elderly patients. *Am. J. Geriatr. Pharmacother.*, **5**, 345–51.

Harris, K. *et al.* (2013) Comparison of electrophysiological data from human-induced pluripotent stem cell-derived cardiomyocytes to functional preclinical safety assays. *Toxicol. Sci.*, **134**, 412–26.

Jacobson, I. *et al.* (2013) Sofosbuvir for hepatitis C genotype 2 or 3 in patients without treatment options. *N. Engl. J. Med.*, **368**, 1867–77.

Katz, A.M. (1993) Cardiac ion channels. *N. Engl. J. Med.*, **328**, 1244–51.

Keating, G.M. (2014) Sofosbuvir: A review of its use in patients with chronic hepatitis C. *Drugs*, **74**, 1127–1146.

Köhler, G.I. *et al.* (2000) Drug-drug interactions in medical patients: effects of in-hospital treatment and relation to multiple drug use. *Int. J. Clin. Pharmacol. Ther.*, **38**, 504–13.

Latini, R. *et al.* (1984) Clinical Pharmacokinetics of Amiodarone. *Clin. Pharmacokinet.*, **9**, 136–156.

Lawitz, E. *et al.* (2014) Sofosbuvir and ledipasvir fixed-dose combination with and without ribavirin in treatment-naive and previously treated patients with genotype 1 hepatitis C virus infection (LONESTAR): An open-label, randomised, phase 2 trial. *Lancet*, **383**, 515–523.

Lawitz, E.J. *et al.* (2013) All-oral therapy with nucleotide inhibitors sofosbuvir and GS-0938 for 14 days in treatment-naive genotype 1 hepatitis C (NUCLEAR). *J. Viral Hepat.*, **20**, 699–707.

Lorberbaum, T. *et al.* (2016) An Integrative Data Science Pipeline to Identify Novel Drug Interactions that Prolong the QT Interval. *Drug Saf.*, **39**, 433–41.

Ma, J. *et al.* (2011) High purity human-induced pluripotent stem cell-derived cardiomyocytes : electrophysiological properties of action potentials and ionic currents. *AJP Hear. Circ. Physiol.*, **301**, 2006–2017.

Nutescu, E. *et al.* (2011) Drug and dietary interactions of warfarin and novel oral anticoagulants: An update. *J. Thromb. Thrombolysis*, **31**, 326–343.

Obergrussberger, A. *et al.* (2014) Automated Patch Clamp Analysis of nAChα7 and NaV 1.7 Channels. *Curr. Protoc. Pharmacol.*, **65**, 11.13.1–11.13.48.

Postma, a V *et al.* (2005) Catecholaminergic polymorphic ventricular tachycardia: RYR2 mutations, bradycardia, and follow up of the patients. *J. Med. Genet.*, **42**, 863–870.

Prueksaritanont, T. *et al.* (2013) Drug-drug interaction studies: regulatory guidance and an industry perspective. *AAPS J.*, **15**, 629–45.

Renet, S. *et al.* (2015) Extreme Bradycardia After First Doses of Sofosbuvir and Daclatasvir in Patients Receiving Amiodarone: 2 Cases Including a Rechallenge. *Gastroenterology*.

Soriano, V. *et al.* (2015) Drug interactions with new hepatitis C oral drugs. *Expert Opin. Drug Metab. Toxicol.*, **11**, 333–341.

Straubhaar, B. *et al.* (2006) The prevalence of potential drug-drug interactions in patients with heart failure at hospital discharge. *Drug Saf.*, **29**, 79–90.

Figure Captions

Figure 1. Sofosbuvir exerts an electrophysiological effect in combination with amiodarone *in vitro*. A) Example FP waveforms for the vehicle control (gray), sofosbuvir (green), amiodarone (red), and the combination of sofosbuvir and amiodarone (blue). B) Percent change from baseline for BP, FPD, FPDc, and AMP in response to the addition of sofosbuvir alone (green). The black line and gray bar indicate the mean ± one standard deviation of the response to the vehicle control. C) Percent change from baseline for BP, FPD, FPDc, and AMP in response to the addition of sofosbuvir and amiodarone (blue). The red line and shaded bar indicate the mean ± one standard deviation of the response to amiodarone for each metric.

Figure 2. GS-331007, the primary circulating metabolite of sofosbuvir, does not interact with amiodarone *in vitro*. A) Example FP waveforms for the vehicle control (gray), GS-331007 (cyan), amiodarone (red), and the combination of GS-331007 and amiodarone (magenta). B) Percent change from baseline for BP, FPD, FPDc, and AMP in response to the addition of GS-331007 alone (cyan). The black line and gray bar indicate the mean +/- one standard deviation of the response to the vehicle control. C) Percent change from baseline for BP, FPD, FPDc, and AMP in response to the addition of the GS-331007 and amiodarone combination (magenta). The red line and shaded bar indicate the mean +/- one standard deviation of the response to amiodarone for each metric. Error bars represent the standard deviation.

Figure 3. Field potential duration is shortened independent of beating rate for the combination of sofosbuvir and amiodarone. A) Measurements of repolarization timing were made after the FPD had stabilized following the onset of pacing. B) Example paced field potential waveforms for dosing with sofosbuvir (green), amiodarone (red), and the drug combination (blue). The paced waveforms from the baseline condition (black) are shown for comparison. All wells were paced at a rate of 2Hz. C) The sofosbuvir and amiodarone combination showed significant shortening of repolarization timing when paced at 2Hz, as compared to the drugs alone or the vehicle control. Error bars represent the standard deviation.

Figure 4. The effect of sofosbuvir with amiodarone is not mediated by block of potassium, sodium, or calcium channels. Raw traces of ionic currents (left) in response to vehicle control (black) and after application of the sofosbuvir (31.6µmol/L) and amiodarone (0.5µmol/L) combination (blue) for A) hERG, B) Nav1.5, and C) Cav1.2 expressed channels. Summarized data (right) are shown for amiodarone (0.5µmol/L) alone and with sofosbuvir (31.6µmol/L) for each channel type. D) Dose response of I_{CaL} block for amiodarone, alone (red) and with sofosbuvir (blue, 31.6µmol/L).

Figure 5. Sofosbuvir and amiodarone impair intracellular calcium handling *in vitro*. A) Raw traces of CaI after application of DMSO, sofosbuvir (3.3µmol/L), amiodarone (0.5µmol/L), and sofosbuvir (3.3µmol/L) with amiodarone (0.5µmol/L). B) Dose response of the calcium transient amplitude, normalized to baseline, for sofosbuvir alone (green). The black line and gray bar indicate the mean +/- one standard deviation of the response to the vehicle control. C) Dose response of the calcium transient amplitude, normalized to baseline, for sofosbuvir with 0.5µmol/L amiodarone (blue). The red line and shaded bar indicate the mean +/- one standard deviation of the response to amiodarone alone.

Figure 6. Sofosbuvir and amiodarone disrupt excitation-contraction coupling *in vitro*. A) Raw traces of IMP before (baseline) and after (30, 120 min) application of sofosbuvir (31.6µmol/L) and amiodarone (0.5µmol/L). Percent change in amplitude of B) IMP and C) FP for 30 and 120 min after compound addition.

Supplementary Data Description

Cardiomyocyte electrophysiology recovers after washout of the sofosbuvir-amiodarone combination

In a separate set of experiments, the field potential was monitored over chronic time points to evaluate the degree to which the electrophysiological effects persisted after washout of the drug combination (Suppl. Fig. 3). The combination of amiodarone and the highest concentration of sofosbuvir exhibited the greatest change in BP from baseline, with dose-dependent changes occurring within 15 minutes post-dose. The dose-dependent decrease in BP remained for the amiodarone and sofosbuvir combination over the 48hr experiment (N=5, $p<0.05$, Wilcoxon rank sum test). After the measurement at the 4hr time point, the sofosbuvir and amiodarone combination was washed out in a subset of wells (magenta). These wells recovered significantly in the 24 and 48hr measurements (N=5, $p<0.05$, Wilcoxon rank sum test).

Electrophysiological effects of sofosbuvir-amiodarone combination are independent of P-gp drug transporter activity

Inhibition of P-glycoprotein (P-gp) is a popular hypothesis for explaining the adverse effects of drug-drug interactions, including those observed with sofosbuvir and amiodarone (Soriano *et al.*, 2015; Back and Burger, 2015). Such an inhibition would be expected to generate increased sofosbuvir concentrations in the plasma and heart. In this study, however, sofosbuvir had no effect on cardiomyocyte physiology at 30x the clinical C_{max}, whereas P-gp effects typically increase C_{max} concentrations by 2-3x (Fenner *et al.*, 2009).

To further test the P-gp hypothesis, we evaluated the electrophysiological effects of combined administration of sofosbuvir and quinidine, a P-gp inhibitor and cardiac anti-arrhythmic drug. Quinidine (300nmol/L) was delivered alone and with sofosbuvir (31.6µmol/L). Quinidine prolonged BP by 10.2±0.8%, FPD by 19.0±2.1%, FPDc by 15.2±1.8%, and reduced AMP by 10.0±5.6%, whereas the combination of quinidine and sofosbuvir prolonged BP by 12.2±1.9%, FPD by 19.8±2.3%, FPDc by 15.3±1.6, and reduced AMP by 6.7±4.2%. None of the endpoints were significantly different between quinidine and the quinidine-sofosbuvir combination (N=4, Wilcoxon rank-sum test).

Finally, we used mass spectrometry measurements to confirm that sofosbuvir was entering the hiPSC-CMs in quantities that were independent of the presence of amiodarone. Indeed, the sofosbuvir uptake (39,382±8,988 arbitrary units, N=2) was unaffected by co-administration with amiodarone at 0.5µmol/L (34,049±2,410 arbitrary units, N=2).

Supplementary Figure Captions

Supplemental Figure 1. The field potential provides a measure of cardiac electrophysiology *in vitro*. hiPSC-CMs form a spontaneously beating syncytium *in vitro*. The cells grow on and interface with electrodes embedded into the culture well substrate of the MEA plate, allowing measurement of the field potential signal. The beat timing, depolarization, and repolarization exhibited by the field potential signal are quantified through the BP, AMP, and FPD, respectively.

Supplemental Figure 2. The electrophysiological effects of sofosbuvir with amiodarone remain with chronic exposure, but recover with washout. A) Change in BP over a 2 hr continuous recording in the MEA assay. Each dot represents a single detected beat. The combination of sofosbuvir and amiodarone has a rapid effect on BP in the MEA assay. B) Change in BP over a 48 hr chronic exposure to sofosbuvir and amiodarone, alone and in combination. The drug combination elicited a dose-dependent decrease in BP that remains over the chronic exposure, but recovered following drug washout in a subset of wells after the 4hr measurement (magenta). Error bars represent the standard deviation.

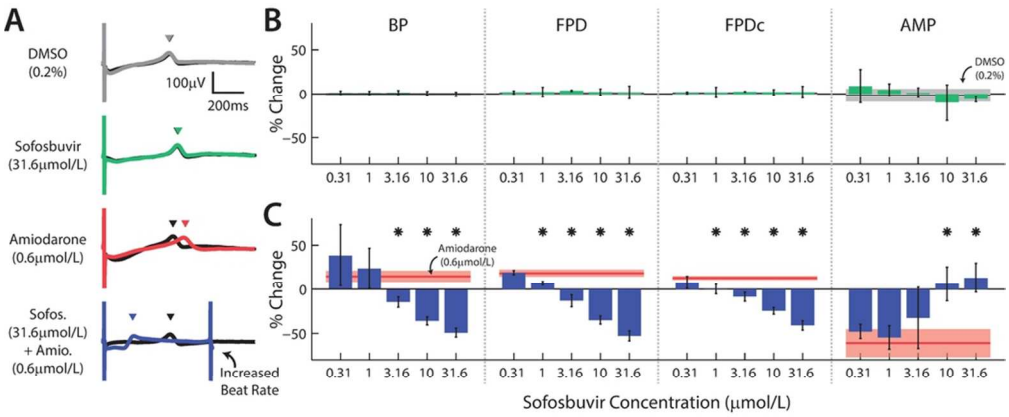

Figure 1

Figure 1. Sofosbuvir exerts an electrophysiological effect in combination with amiodarone in vitro. A) Example FP waveforms for the vehicle control (gray), sofosbuvir (green), amiodarone (red), and the combination of sofosbuvir and amiodarone (blue). B) Percent change from baseline for BP, FPD, FPDc, and AMP in response to the addition of sofosbuvir alone (green). The black line and gray bar indicate the mean ± one standard deviation of the response to the vehicle control. C) Percent change from baseline for BP, FPD, FPDc, and AMP in response to the addition of sofosbuvir and amiodarone (blue). The red line and shaded bar indicate the mean ± one standard deviation of the response to amiodarone for each metric.

88x41mm (300 x 300 DPI)

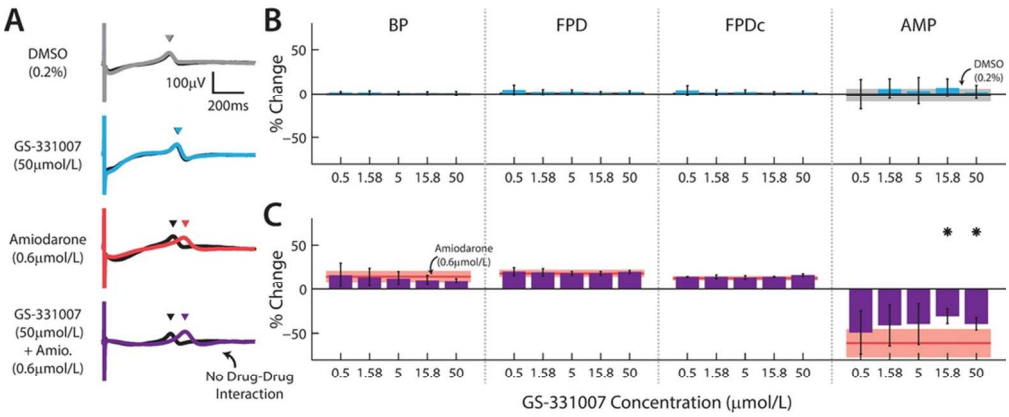

Figure 2

Figure 2. GS-331007, the primary circulating metabolite of sofosbuvir, does not interact with amiodarone in vitro. A) Example FP waveforms for the vehicle control (gray), GS-331007 (cyan), amiodarone (red), and the combination of GS-331007 and amiodarone (magenta). B) Percent change from baseline for BP, FPD, FPDc, and AMP in response to the addition of GS-331007 alone (cyan). The black line and gray bar indicate the mean +/- one standard deviation of the response to the vehicle control. C) Percent change from baseline for BP, FPD, FPDc, and AMP in response to the addition of the GS-331007 and amiodarone combination (magenta). The red line and shaded bar indicate the mean +/- one standard deviation of the response to amiodarone for each metric. Error bars represent the standard deviation.

88x41mm (300 x 300 DPI)

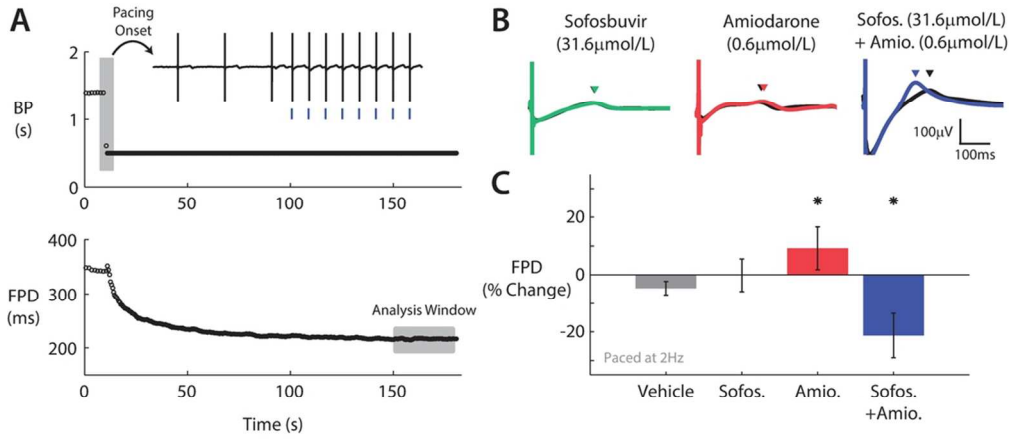

Figure 3

Figure 3. Field potential duration is shortened independent of beating rate for the combination of sofosbuvir and amiodarone. A) Measurements of repolarization timing were made after the FPD had stabilized following the onset of pacing. B) Example paced field potential waveforms for dosing with sofosbuvir (green), amiodarone (red), and the drug combination (blue). The paced waveforms from the baseline condition (black) are shown for comparison. All wells were paced at a rate of 2Hz. C) The sofosbuvir and amiodarone combination showed significant shortening of repolarization timing when paced at 2Hz, as compared to the drugs alone or the vehicle control. Error bars represent the standard deviation.

93x46mm (300 x 300 DPI)

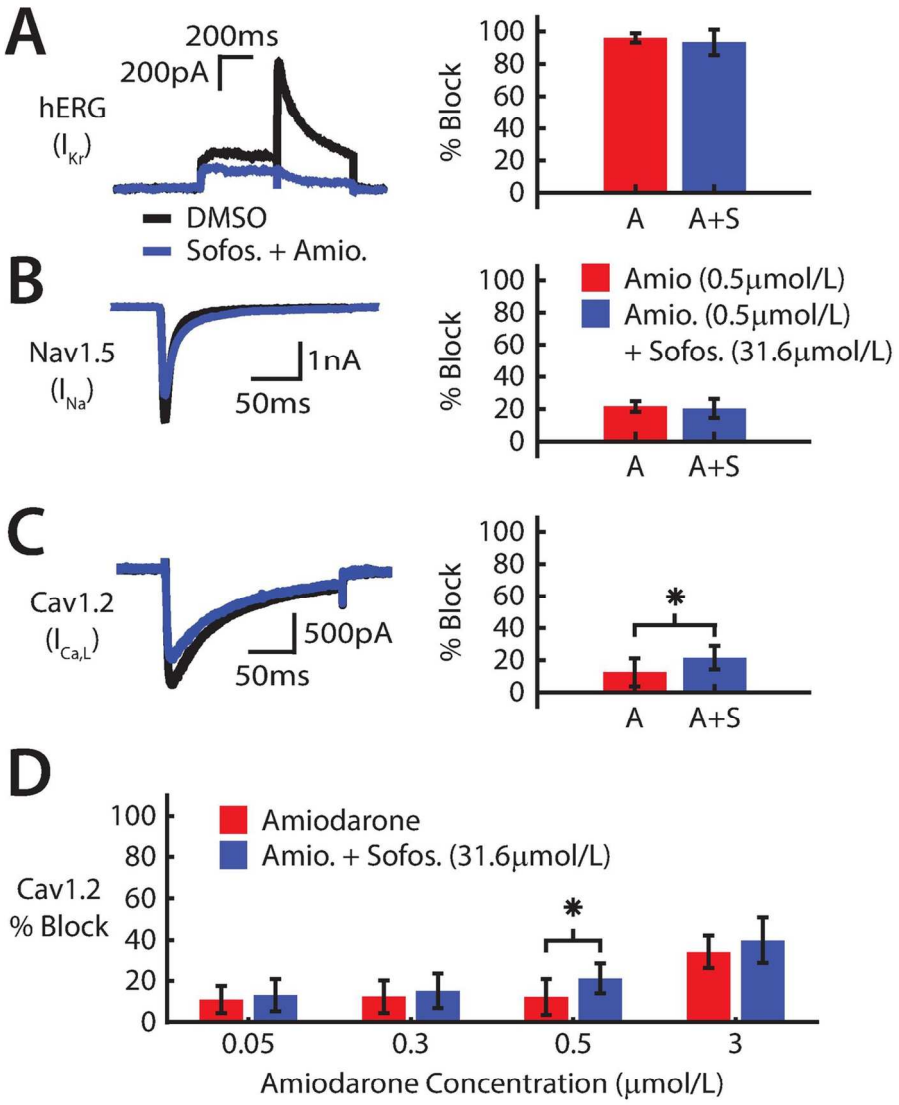

Figure 4

Figure 4. The effect of sofosbuvir with amiodarone is not mediated by block of potassium, sodium, or calcium channels. Raw traces of ionic currents (left) in response to vehicle control (black) and after application of the sofosbuvir (31.6µmol/L) and amiodarone (0.5µmol/L) combination (blue) for A) hERG, B) Nav1.5, and C) Cav1.2 expressed channels. Summarized data (right) are shown for amiodarone (0.5µmol/L) alone and with sofosbuvir (31.6µmol/L) for each channel type. D) Dose response of ICaL block for amiodarone, alone (red) and with sofosbuvir (blue, 31.6µmol/L).

110x149mm (300 x 300 DPI)

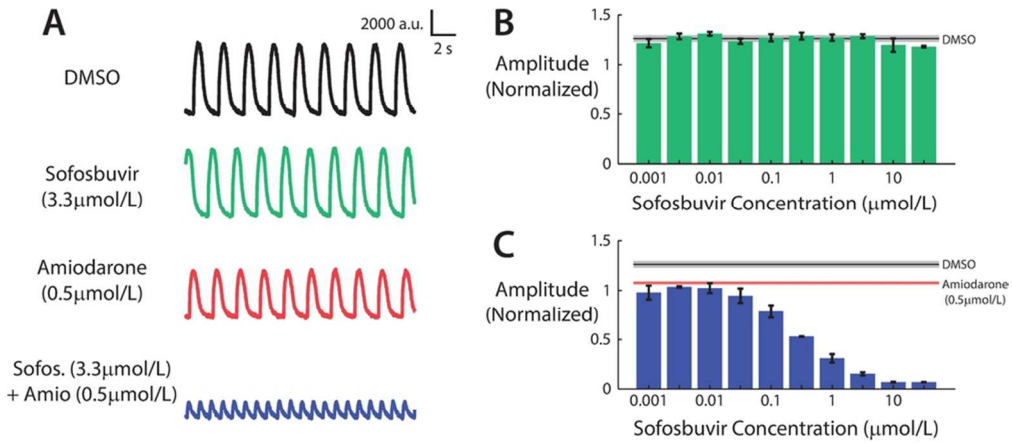

Figure 5

Figure 5. Sofosbuvir and amiodarone impair intracellular calcium handling in vitro. A) Raw traces of CaI after application of DMSO, sofosbuvir (3.3µmol/L), amiodarone (0.5µmol/L), and sofosbuvir (3.3µmol/L) with amiodarone (0.5µmol/L). B) Dose response of the calcium transient amplitude, normalized to baseline, for sofosbuvir alone (green). The black line and gray bar indicate the mean +/- one standard deviation of the response to the vehicle control. C) Dose response of the calcium transient amplitude, normalized to baseline, for sofosbuvir with 0.5µmol/L amiodarone (blue). The red line and shaded bar indicate the mean +/- one standard deviation of the response to amiodarone alone.

84x43mm (300 x 300 DPI)

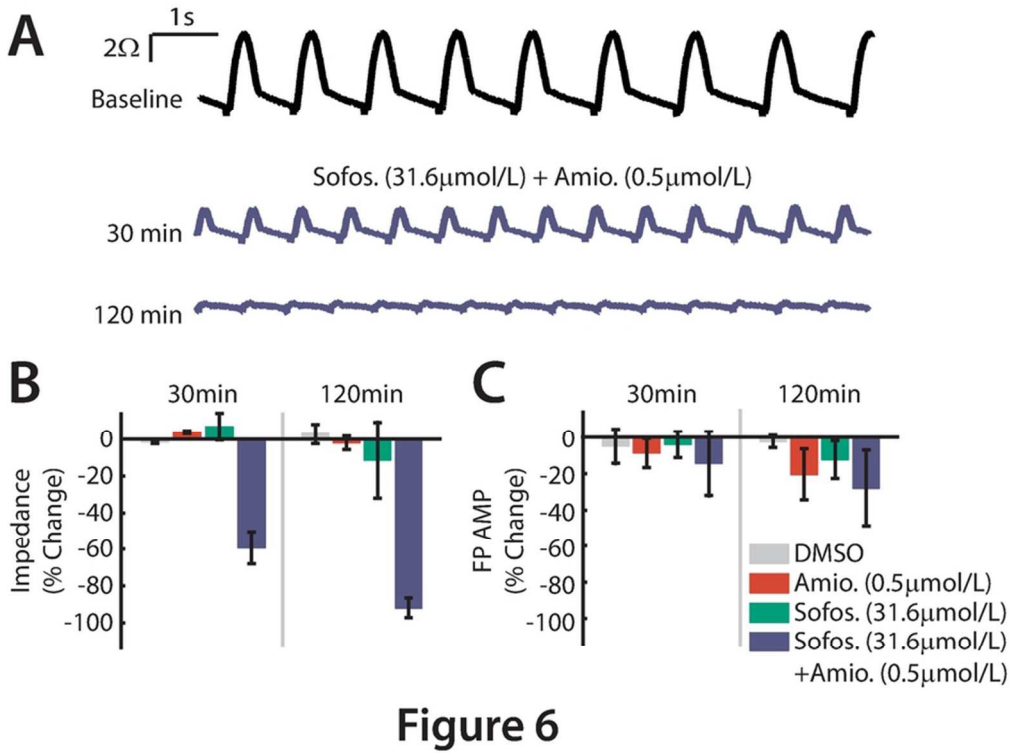

Figure 6

Figure 6. Sofosbuvir and amiodarone disrupt excitation-contraction coupling in vitro. A) Raw traces of IMP before (baseline) and after (30, 120 min) application of sofosbuvir (31.6µmol/L) and amiodarone (0.5µmol/L). Percent change in amplitude of B) IMP and C) FP for 30 and 120 min after compound addition.

79x59mm (300 x 300 DPI)